ISSN 0027-1349, Moscow University Physics Bulletin, 2015, Vol. 70, No. 6, pp. 473–478. © Allerton Press, Inc., 2015.
Original Russian Text © F.B. Khlebnikov, A.N. Bogolyubov, V.S. Solosin, N.E. Shapkina, 2015, published in Vestnik Moskovskogo Universiteta. Fizika, 2015, No. 6, pp. 43–48.

THEORETICAL AND MATHEMATICAL PHYSICS

The Mathematical Simulation of a Diffracted Field in the Target Area of a Mirror Collimator

F. B. Khlebnikov[a], A. N. Bogolyubov[a], V. S. Solosin[b], and N. E. Shapkina[a]

[a] *Moscow State University, Moscow, 119991 Russia*

[b] *Federal State Research Institute for Theoretical and Applied Electromagnetics (ITAE), Russian Academy of Sciences, Moscow, 125412 Russia*

e-mail: mnfkhl@gmail.com

Received July 14, 2015; in final form, September 1, 2015

Abstract—A mathematical model of a mirror collimator with rounded edges is developed. The problem of calculating electromagnetic field components in the target area is solved by the method of integral equations. The results of numerical computations are presented.

Keywords: mathematical simulation, mirror collimator.

DOI: 10.3103/S0027134915060119

INTRODUCTION

An important problem of practical electrodynamics is obtaining a field with a structure that is similar to the field of a plane electromagnetic wave in a specified volume. In particular, this task is significant for problems that are associated with radiolocation in studying the process of body irradiation that is emitted from a remote source. Similar problems arise on measuring antenna directivity patterns. In order to generate a field with a structure close to a plane wave, the studied body must be placed at a reasonably large distance from the source in the Fraunhofer zone, or the far field, as it is called in radiolocation. This can be done on open testbeds but there the interpretation of findings can be significantly complicated by the weather conditions, characteristics of the environment, and other factors. Another investigation method is the formation of a field that is similar to a plane wave field in a closed space of a measuring laboratory. In the latter case, collimators, i.e., devices that convert a spherical wave into a plane one, are used. Measuring benches that are based on an anechoic chamber where a plane field is formed by a collimator are called compact ranges [1].

As in optics, there are two types of collimators in electrodynamics, i.e., lens-based and mirror-based. There are also other schemes for the generation of a plane field, in particular, using simple antenna arrays and holographic schemes based on shadow masks, such as a Fresnel zone plate.

The limited use of collimators based on dielectric lenses is due to the high technical complexity of lens manufacturing, in particular, the homogeneity requirements for the material of the lens and precision machining of its surface; therefore, most collimators for compact ranges are mirror collimators.

The target area of a collimator is an area where the reflected field can with reasonable accuracy be considered a plane wave field. It is a limited cylindrical region, whose axis is parallel to the axis of the paraboloid. The dimensions of the target area depend on the frequency of the incident wave and the size of the mirror while the mirror of the collimator must be large enough to reduce the influence of edge diffraction effects. Usually, the transverse size of the collimator is approximately twice the size of the target area. The field inhomogeneity in the target area of the compact range can be attributed to the collimator design, the properties of the radar-absorbing material, its location in the anechoic chamber, and multipath waves with auxiliary devices.

1. EDGE EFFECTS IN MIRROR COLLIMATORS

One of the most important problems of collimators is to reduce the influence of edge diffraction effects in the field that is generated in the target area of the collimator. The attempts to reduce this impact date back to the emergence of the first compact ranges [2]. One example is the design of widely applied collimators that use reflectors with serrated edges. The production technology for such collimators has been constantly improving and today it can reduce the field inhomogeneity in the target area to approximately 1 dB.

The increasing requirements for the precision of measurements stimulated the development of collimators that provide greater measurement accuracy as

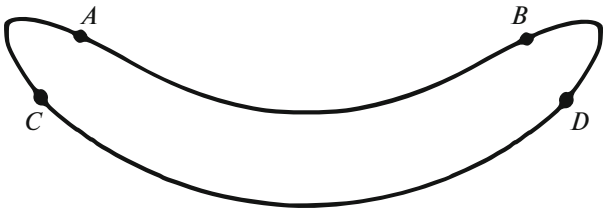

Fig. 1. The cross section of a collimator with rounded edges.

early as the 1980s. An example of such a collimator design is a mirror with a rounded edge [3, 4]. In the two-dimensional case, such a mirror is designed as a combination of its parabolic part and fillets on the edges that deflect the beams that are incident on the edges, thus preventing them from penetration into the target area. An example of such roundings is an elliptical fillet.

The model that was proposed in [4] was based on a three-dimensional variant of a symmetrical mirror with rounded edges and a complex contour of the parabolic and rounded parts. Investigation by the methods of physical optics enabled the authors to propose a nontrivial nonconvex curvilinear integration contour shaped like a four-pointed star [5].

In order to assess the behavior of the collimator field with curved edges in the target area, numerous calculations were carried out. In [6], the results of numerical experiments are presented that were conducted by the method of the geometric theory of diffraction. Its findings are in a sufficiently good agreement with the results that have been obtained by the methods of physical optics.

The study [7] presented the results of an experiment based on the installation of additional scattering plates on an already functioning collimator located at Ohio State University, United States. A smoothing "skirt" was specially manufactured by one of NASA-supported centers. As should be expected, this modification resulted in significant smoothing of the field in the target area. This experiment clearly demonstrates that it is possible to modify a collimator with serrated edges using such devices but this opportunity is rarely used in practice because the manufacturing of the "skirt" and revamping of the chamber are complex and difficult.

More detailed theoretical studies of this subject include, for example, such publications as [8, 9]. The first of these considers the design of a collimator with a specially shaped serrated edge with an angle of scallops, in accordance with the techniques of geometric optics, chosen so as to redirect the beams that are reflected from the edges away from the target area of the collimator. Despite this, the comparison between this collimator and the one that was designed according to [4] shows that rounded edges make it possible to obtain a much smoother field in the target area. Collimators with a rounded edge are widely used in practice [10].

It should be noted that the field in the target area could also be effectively improved by using high-quality radar absorbing materials. Currently, these materials are widely used to cover walls, floors, ceilings, and devices inside the anechoic chamber [11, 12]. A wide variety of radar-absorbing materials exist, both narrow-band ones based on resonance phenomena and more universal broadband materials [13–16].

2. MATHEMATICAL SIMULATION OF A COLLIMATOR FIELD

In this work, a collimator with a flanged edge is studied using mathematical simulation. The finite-element method is an effective solution technique for such problems [17]. In our study, we apply the no-less-effective method of integral equations. Let us consider the model problem. Let an electromagnetic wave from a linear source be incident on a perfectly conducting infinite cylindrical surface with a cross section of a complex shape (Fig. 1), whose axis is parallel to the source. Here, the surface AB, which is located close to the source, is a parabolic cylindrical surface, the focus of which coincides with the source; the surface CD is a circular cylindrical surface, and the surfaces AC and BD, which join the first two surfaces, are elliptic cylindrical surfaces. It should be required that the part of the studied surface that faces the source would be at least a surface of the type C^1.

The coordinate system is chosen so that the z axis is directed along the axis of the cylinder, so that the problem can be considered as a two-dimensional problem in the xy plane. Here, we choose the focus of the parabola formed by the intersection of the cylinder and the xy plane as the origin of the coordinates, the y axis will be directed along the axis of the parabola, and the source will be placed at the origin of the coordinates. The equation the ellipse (e.g., AC) is written as

$$x^2 + 2b_{12}xy + b_{22}y^2 + 2b_{13}x + 2b_{23}y + b_{33} = 0. \quad (1)$$

Imposing the requirement that the resulting cross-sectional contour be sufficiently smooth at the points of the curve junctions, we write the condition for the smooth junction of the ellipse AC and parabola AB

$$\begin{gathered} 4dl^3b_{12} + l^4b_{22} + 8d^2lb_{13} + 4dl^2b_{23} + 4d^2b_{33} + 4d^2l^2 = 0, \\ 4dl^2b_{12} + l^3b_{22} + 2dlb_{23} + 4d^2b_{13} + 4d^2l = 0, \quad (2) \\ (1+2l)\,db_{12} + l^2b_{22} + 2b_{32} + 2d = 0. \end{gathered}$$

Here, l is the x-coordinate of the junction point and d is the focal length of the parabola. With allowance for these conditions, we obtain a family of ellipses with two free parameters.

The chamber is assumed to be sufficiently large compared with the investigated object. At such a con-

dition, we neglect the influence of the chamber walls and only consider the field that is scattered by the mirror of the collimator. The diffracted field can be represented as a superposition of the electric and magnetic fields and can be written using the Borgnis functions.

For an electric field, we consider the Helmholtz equation for the Borgnis function, u [18], (here and below it is assumed that time dependence occurs in the form $e^{i\omega t}$)

$$\Delta u + k^2 u = f(M) \tag{3}$$

with boundary conditions

$$u\big|_C = 0 \tag{4}$$

and the radiation condition at infinity

$$\left.\frac{\partial u}{\partial r} + iku\right|_{r\to\infty} = o\left(\frac{1}{\sqrt{r}}\right). \tag{5}$$

Here, C is the contour that is obtained by the above-described smooth junction of curves (Fig. 1) and k is the wave number. The problem for the magnetic field has the same form with accuracy up to the boundary condition. The field of a magnetic type satisfies the equation

$$\Delta u + k^2 u = f(M) \tag{6}$$

with Neumann boundary conditions on the boundary of the contour

$$\left.\frac{\partial u}{\partial n}\right|_C = 0, \tag{7}$$

$$\left.\frac{\partial u}{\partial r} + iku\right|_{r\to\infty} = o\left(\frac{1}{\sqrt{r}}\right). \tag{8}$$

In this case, for the components of the electromagnetic field we have

$$E_x = -\frac{i}{\omega\varepsilon}\frac{\partial u(x,y)}{\partial y}, \quad E_y = \frac{i}{\omega\varepsilon}\frac{\partial u(x,y)}{\partial x}, \tag{9}$$

$$E_z = H_x = H_y = 0,\ H_z = u(x,y). \tag{10}$$

We introduce Green's function $g(M,P)$ of the free space as the solution of equation

$$\Delta g(M,P) + k^2 g(M,P) = -2\pi\delta(r_{MP}) \tag{11}$$

with conditions of radiation at infinity and with a solution in the form of the zeroth-order Hankel function of the second kind

$$g(M,P) = -\frac{i\pi}{2}H_0^{(2)}(kr_{MP}). \tag{12}$$

For the fields of electric and magnetic type, we use the properties of potentials of single and double layer and obtain the following relations:

$$\frac{1}{2\pi}\int_C \frac{\partial u(P)}{\partial n} g(M,P)ds = -u_0(M), \tag{13}$$

$$\frac{1}{2}u(M) + \frac{1}{2\pi}\int_C u(P)\frac{\partial g(M,P)}{\partial n}ds = u_0(M), \tag{14}$$

where M is the observation point on the surface of the conductor, P is the source point, and the function $u_0(M)$ characterizes the incident wave. For the case of the surface excitation by a filament of an electric current, the equation for the current on the conductor surface has the form

$$H_0^{(2)}(kr_M) = -\frac{1}{2\pi}\oint_C J(P)H_0^{(2)}\left(k\left|r_M - r_P\right|\right)ds. \tag{15}$$

Knowing the current distribution, we can calculate the field in the target area of the collimator by the formula

$$H_z(M) = \frac{1}{2\pi}\oint_C J(P)H_0^{(2)}(kr_{P,M})dl_P.$$

The problem is solved numerically by the collocation method.

We proceed to the discrete analog of Eq. (15) by dividing the integration contour by N arcs C_n. By representing the integral in (15) as a sum of integrals over sections $C_n, C = \sum C_n$ we obtain a system of linear equations in currents J_n

$$H_0^{(2)}(kr_m) = -\frac{1}{2\pi}\sum_{n=1}^{N} J_n \int_{C_n} H_0^{(2)}\left(k\left|r_M - r_P\right|\right)ds, \tag{16}$$

in which the matrix coefficients are integrals of the Hankel function

$$M_{m,n} = -\frac{1}{2\pi}\int_{C_n} H_0^{(2)}\left(k\left|r_M - r_P\right|\right)ds. \tag{17}$$

Since the selected arcs C_n are small, the Hankel function can be approximated by the piecewise constant function

$$M_{m,n} = -\frac{1}{2\pi}\Delta\cdot H_0^{(2)}\left(k\sqrt{(x_m - x_n)^2 + (y_m - y_n)^2}\right) \tag{18}$$

at $m \neq n$. For $m = n$

$$M_{n,n} = -\frac{1}{2\pi}\Delta\left(1 - i\frac{2}{\pi}\ln\left(\frac{\gamma k\Delta_n}{4e}\right)\right), \tag{19}$$

where Δ_n designates the lengths of the contour arcs C_n, γ is the Euler constant, and e is the base of the natural logarithm. Thus, the current distribution on a cylinder of an arbitrary shape can be obtained as a solution of a system of linear equations

$$M_{m,n}J_n = b_m \tag{20}$$

with a symmetric matrix.

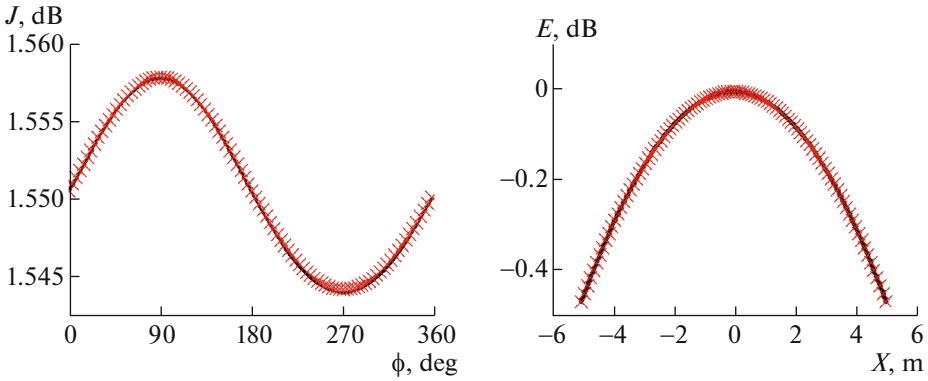

Fig. 2. The current distribution on a circular cylinder and its field in the target area.

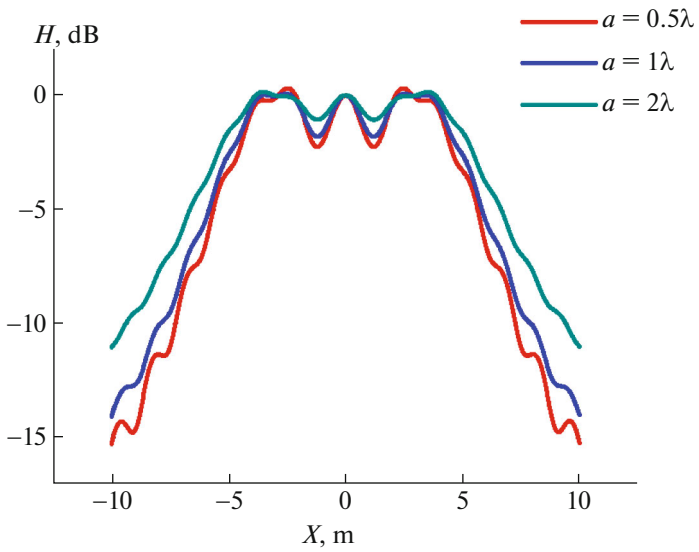

Fig. 3. A field reflected by a plane mirror with fillets of different sizes.

Then, the sought field has the form

$$U_{app} = \frac{1}{2\pi}\sum_{n} J_n H_0^{(2)}(kr_{n,m}) \cdot \Delta_n. \qquad (21)$$

Based on the above-presented model, a program has been developed in the Mathcad environment and a series of calculations has been carried out, in particular, for several characteristic limiting cases [19].

In order to validate the model, calculations were performed for the simplest case of a cylinder with a circular cross section resulting from the contour that is shown in Fig. 1 when the length of the arc AB tends to zero. The radiation source is set at a great distance. In this case, the currents that are induced on the paraboloid, as well as the scattered field, are calculated analytically [20]. As shown by a numerical experiment, the results that are obtained by this mathematical model are in good agreement with the analytical solution (Fig. 2).

In the limiting case, which is more important from the practical viewpoint, the focal length of the parabola tends to infinity. In this case, the front and rear walls of section z = const degenerate into segments of straight lines. Since the radiation source should be placed in the focus of the parabolic arc, it also becomes infinitely remote, and the wave incident on the body becomes planar. Several numerical experiments have been conducted with varying rounding sizes with respect to the wavelength. The selected value that characterizes the rounding size was the semimajor axis of the ellipse a.

In the graph that is shown in Fig. 3, different curves correspond to different sizes of the main axis of the rounding, a, with respect to the wavelength, λ. It is clearly seen that the increase in the rounding size has a positive effect on the field in the target area, significantly suppressing its inhomogeneities.

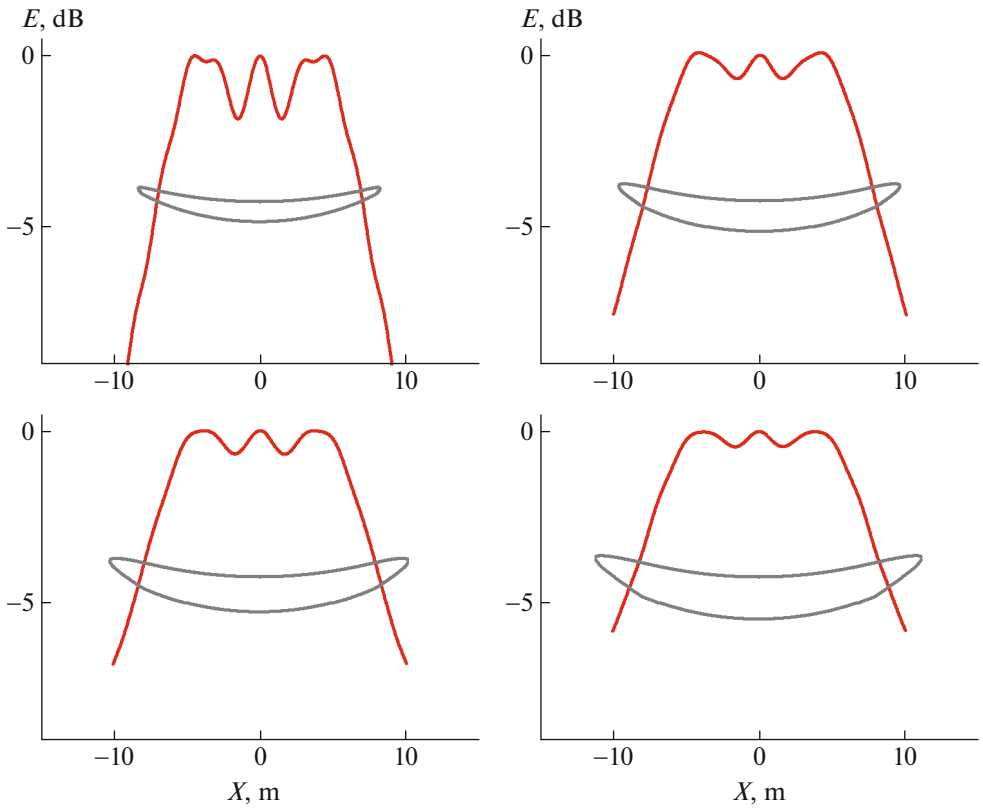

Fig. 4. A parabolic mirror with rounded edges and its field in the target area.

This is accompanied by the simultaneous increase in the field outside the target area. Although this field is not treated in detail in the context of our problem, with regard to practical measurements, this effect can affect the accuracy of experiments in the anechoic chamber due to multiple reflections from the walls.

Investigation into the general case where the arc AB is not degenerate would be of great interest. In contrast to the previous case, the family of possible fillets is multivariable, as suitable ellipses may have different tilt angles of the axes and coordinates of the point of junction with the parabolic part of the contour. Nevertheless, the overall trend remains the same, i.e., under otherwise equal conditions, the increase in the rounding size improves the field in the target area but also increases the amplitude of the field outside it.

As can clearly be seen from Fig. 4, which presents the field distributions for various mirror profiles that differ in the sizes of the fillets, making use of sufficiently large rounding effectively suppresses most of the diffraction effects. While in the first graph, which corresponds to the smallest fillets, there are additional maxima in the target area, these extreme points disappear in the second graph and further the field smoothness constantly improves.

CONCLUSIONS

Despite its simplicity, the developed mathematical model for the two-dimensional case enables qualitative assessment of a field in the target area of a mirror collimator with rounded edges. The conducted numerical experiments show both the advantages and disadvantages of such collimators: the advantages include a substantial improvement in the reflected field; however, it requires a sufficiently large size of the rounded edges.

REFERENCES

1. N. P. Balabukha, A. S. Zubov, and V. S. Solosin, *Small Test Sites for the Measurement of Scattering Properties of Objects* (Moscow, 2007) [in Russian].
2. W. Emerson, IEEE Trans. Antennas Propag. **21**, 484 (1973).
3. C. Pistorius and D. Burnside, IEEE Trans. Antennas Propag. **35**, 342 (1987).
4. I. Gupta, K. Ericsen, and W. Burnside, IEEE Trans. Antennas Propag. **38**, 853 (1990).
5. T. Lee, W. Burnside, and I. Gupta, presented at *The 26th Annual Meeting of the Antenna Measurement Techniques Association* (Stone Mountain Park, USA, 2004).
6. S. Ellington, I. Gupta, and W. Burnside, IEEE Trans. Antennas Propag. **38**, 1969 (1990).

7. W. Burnside, M. Gilreath, B. Kent, and G. Clerici, IEEE Trans. Antennas Propag. **35**, 176 (1987).
8. A. Munoz-Acevedo, S. Burgos, and M. Sierra-Castaner, in *Proc. 5th European Conf. on Antennas and Propagation* (IEEE, 2011), p. 3586.
9. T. Lee and W. Burnside, IEEE Trans. Antennas Propag. **44**, 87 (1996).
10. M. Shields and A. Fenn, Lincoln Lab. J. **16** (2), 381 (2007).
11. J. Appel-Hansen, IEEE Trans. Antennas Propag. **21**, 490 (1973).
12. A. V. Nikitenko, A. S. Zubov, and N. E. Shapkina, Math. Models Comput. Simul. **7**, 134 (2015).
13. H. Severin, IEEE Trans. Antennas Propag. **4**, 385 (1956).
14. W. Sun, K. Liu, and C. Balanis, IEEE Trans. Antennas Propag. **44**, 798 (1996).
15. M. Amano and Y. Kotsuka, IEEE Trans. Microwave Theory Tech. **51**, 238 (2003).
16. M. Johansson, C. Holloway, and E. Kuester, IEEE Trans. Antennas Propag. **53**, 728 (2005).
17. A. N. Bogolyubov, N. A. Bogolyubov, and A. G. Sveshnikov, Fiz. Osn. Priborostr. **2** (1), 10 (2013).
18. A. G. Sveshnikov and I. E. Mogilevskii, *Mathematical Problems of Diffraction Theory* (Moscow, 2010) [in Russian].
19. F. B. Khlebnikov, N. E. Shapkina, and V. S. Solosin, presented at *The 12th Annual Sci. Conf. of the Institute of Theoretical and Applied Electrodynamics* (Moscow, Russia, 2011).
20. F. B. Khlebnikov, presented at *The 5th Int. Conf. "Acoustooptic and Radar Techniques for Measurement and Data Processing"* (Suzdal, Russia, 2012).

Translated by I. Pertsovskaya